Energy & Buildings 285 (2023) 112923

Contents lists available at ScienceDirect

Energy & Buildings

journal homepage: www.elsevier.com/locate/enb

Experimental validation of a state-of-the-art model predictive control approach for demand side management with a hot water heat pump

Christian Baumann [a,b], Gerhard Huber [a,b], Jovan Alavanja [a,b], Markus Preißinger [a,b], Peter Kepplinger [a,b,*]

[a] illwerke vkw Endowed Professorship for Energy Efficiency, Research Center Energy, Vorarlberg University of Applied Sciences, Dornbirn, Austria
[b] Josef Ressel Centre for Intelligent Thermal Energy Systems, Vorarlberg University of Applied Sciences, Dornbirn, Austria

ARTICLE INFO

Article history:
Received 8 September 2022
Revised 2 December 2022
Accepted 17 February 2023
Available online 24 February 2023

Keywords:
Demand side management
Demand response
Heat pump
Model predictive control (MPC)
Thermal energy storage

ABSTRACT

Hot water heat pumps are well suited for demand side management, as the heat pump market faced a rapid growth in the past years with the trend to decentralized domestic hot water use. Sales were accelerated through wants and needs of energy conservation, energy efficiency, and less restrictive rules regarding *Legionella*. While in literature the model predictive control potential for heat pumps is commonly shown in simulations, the share of experimental studies is relatively low. To this day, experimental studies considering solely domestic hot water use are not available. In this paper, the realistic achievable model predictive control potential of a hot water heat pump is compared to the standard hysteresis control, to provide an experimental proof. We show for the first time, how state-of-the-art approaches (model predictive control, system identification, live state estimation, and demand prediction) can be transferred from electric hot water heaters to hot water heat pumps, combined, and implemented into a real-world hot water heat pump setup. The optimization approach, embedded in a realistic experimental setting, leads to a decrease in electric energy demand and cost per unit electricity by approximately 12% and 14%, respectively. Further, an increase in efficiency by approximately 13% has been achieved.

1. Introduction

The heat pump (HP) market in the EU faced a growth of 81% in the past years (2015–2020) [1], mostly driven by air-source HPs. With this number in mind, one might ask if HPs with thermal energy storages (TES) can provide additional flexibility for the integration of renewable energy generation. In this context, three use cases are possible: 1) Space heating (SH), 2) domestic hot water (DHW), and 3) a combination of both. In multi-family residential complexes, decentralized DHW use increases in importance because of energy conservation, energy efficiency, and less restrictive rules regarding *Legionella* [2]. Increasing sales of domestic hot water heat pumps (HWHP) by +15% in Germany (2020–2021) show the promising trend of this technology [3].

To use the potential of HWHPs for renewable energy integration, demand shifting (DSM) via model predictive control (MPC) is a promising approach compared to common rule-based approaches, like standard hysteresis control (HYS) [4]. In literature, MPC is of particular interest due to its high versatility in handling multiple objectives [5,6]. Compared to HYS, MPC focuses on incentives such as day-ahead spot market prices [2,7].

In literature, MPC is applied in both, simulations and experimental studies.

Simulation studies commonly compare rule-based control strategies of HPs like HYS to MPC approaches, assuming perfect system knowledge. Mostly HPs with TES for SH and/or DHW in residential buildings are considered. Investigations considering both, DHW and SH operation, report cost savings of 11 – 24% [8,9]. Results of studies with configurations for SH use only align with that, and report cost and electric energy savings of 5 – 34% and 13 – 16%, respectively [10–13]. However, DHW configurations present a higher impact on the potential, showing cost savings up to 65% and energy savings of 20 – 32% [14,15].

In contrast to the variety of simulation studies, experimental studies are rare.

Kuboth et al. [16,17] operated two identical test rig setups in parallel. Every test rig consisted of an HP with 500 liter TES for SH use. In a short-term investigation (5 days) [16] and long-term investigation (125 days) [17], MPC was compared to a HYS strategy. The short-term investigation showed that the HP operation was shifted from night to the morning and afternoon hours, while

* Corresponding author at: illwerke vkw Endowed Professorship for Energy Efficiency, Research Center Energy, Vorarlberg University of Applied Sciences, Hochschulstraße 1, Dornbirn 6850, Austria.
E-mail address: peter.kepplinger@fhv.at (P. Kepplinger).

https://doi.org/10.1016/j.enbuild.2023.112923
0378-7788/

Nomenclature

Roman letters

c	real time price (EUR/MWh)
C_{el}	costs per unit electricity (EUR/MWh)
C_{th}	costs per unit heat (EUR/MWh)
c_w	thermal capacity of water (kJkg^{-1}K^{-1})
C	total thermal capacitance (JK^{-1})
COP	coefficient of performance (–)
P_{el}	electric power HP compressor (W)
$\dot{Q}_{dem}$	hot water energy demand rate (W)
$\dot{Q}_{loss}$	energy losses to environment (W)
$\overline{T}$	average water temperature (K)
T_{dem}	fixed draw-off temperature (K)
T_{max}	maximal average water temperature in storage (K)
T_{min}	minimal average water temperature in storage (K)
T_{in}	inlet water temperature (K)
T_{out}	outlet water temperature (K)
T_0	initial average water temperature in storage (K)
T_∞	ambient temperature (K)
T_{tw}	thermal well temperature (K)
t	time (s)
u	switch signal (–)
UA	overall heat transfer characteristics (WK^{-1})
$\dot{V}$	volume flow rate (m^{3}s^{-1}
$\dot{W}_{el}$	electrical energy input rate (W)

Calligraphic letters

$\mathcal{T}_{HC}$	set of discrete points in time (–)

Greek letters

ϱ	water density (kgm^{-3})

Super- and subscripts

$\tilde{x}$	estimation superscript (–)
x^*	prediction superscript (–)

Abbreviations

DDP	data-driven probabilistic approach
DHW	domestic hot water
DSM	demand side management
EHWH	electric hot water heater
HC	heating cycles
HP	heat pump
HWHP	hot water heat pump
HYS	hysteresis control
LP	linear optimization problem
MPC	model predictive control
PEM	prediction error method
PP	perfect prediction
RMSE	root mean squared error
RTP	real time price
SH	space heating
TES	thermal energy storage

a cost reduction of 34% and an efficiency increase of 22% was achieved. The long-term investigation verified the method and lead to the results showing a cost reduction of 9%, a decrease in electrical energy consumption of 4% and an efficiency increase of 5%.

The test rig of Péan et al. [18] comprises an HP for SH and DHW including a 200 liter TES for DHW use only. A MPC approach is compared to a HYS strategy. Within a three-day test period, results showed a cost reduction of 7% and a minor increase in electrical energy consumption. However, the MPC strategy often failed to shift the DHW loads because of hardware control problems. Although potential solutions to overcome this problem are implied, the DHW potential could not be sufficiently proved.

To summarize: Despite the MPC potential of DHW use with heat pumps is stated in literature [6,19,20], to this day, no experimental validation in a realistic setting is available.

However, similar approaches with MPC focussing on DHW were already investigated in the field of electric hot water heaters (EHWH). Demand forecasting was also already investigated in that field. A good overview is provided in the PhD theses of two main scientist, namely Kepplinger [21] and Ritchie [22].

Kepplinger et al. [23] proofed the MPC potential in an experimental setup comprising an EHWH with 150 liter TES, and emphasized the importance of accurate demand forecasting. To obtain more accurate DHW profiles, and to present an alternative to standard demand profiles, a data-driven probabilistic (DDP) approach was developed by Ritchie et al. [24].

Summarized, literature lacks an experimental study on HP with TES for DHW use. The study should compare a MPC to a HYS strategy, considering realistic boundary conditions.

We want to overcome this lack and contribute the following aspects to the community:

- The transfer and combination of state-of-the-art approaches of EHWH to HWHP (MPC, system identification, live state estimation, and demand prediction).
- An experimental proof of the MPC potential of HWHPs by comparison of HYS and MPC covered in a realistic setting.
- Quantification of the savings and the DSM potential achievable by a state-of-the-art prediction method in a realistic setting.

We achieve this by developing an experimental setup with an air-source HWHP including 200 liter TES (cf. Section 2) featuring state-of-the-art approaches for MPC, system identification, live state estimation, and demand prediction [24–26] (cf. Section 3). All novel approaches are implemented together for the first time in a real-world environment.

2. Experimental setup

The test rig comprises an indoor installed off-the-shelf 200 liter air-source HWHP (type Austria Email Explorer Evo 2 [27]). The standard control of the HP system is based on a hysteresis with 7 Kelvin, where 55°C and 48°C represent the upper and the lower threshold value, respectively, implemented using the manufacturer's thermal well temperature sensor. The HYS itself serves as a benchmark reference for the comparison to the MPC.

We equipped the HWHP with sensors and actuators as shown in Fig. 1. Temperatures T_{tw}, T_{in}, T_{out} and ambient temperature T_∞ are measured via K-Type thermocouples. The thermal well temperature sensor T_{tw} is non-invasively arranged in the storage next to the manufacturer's sensor. The water inlet temperature sensor T_{in} is installed in the inlet pipe. The hot water outlet temperature T_{out} is measured in the outlet pipe next to the top of the storage. Electric power consumption $\dot{W}_{el}$ is recorded by a power meter (type Lumel N27P [28]) with a maximum measurable power of 2.88 kW and a relative error in accuracy of ±0.5%. Volume flow rate $\dot{V}$ is measured using a magnetic inductive flow meter (type ifm electronic SM6000 [29]) with a relative error in accuracy of ±2%. The hot water demand $\dot{Q}_{dem}$ is determined by calculation

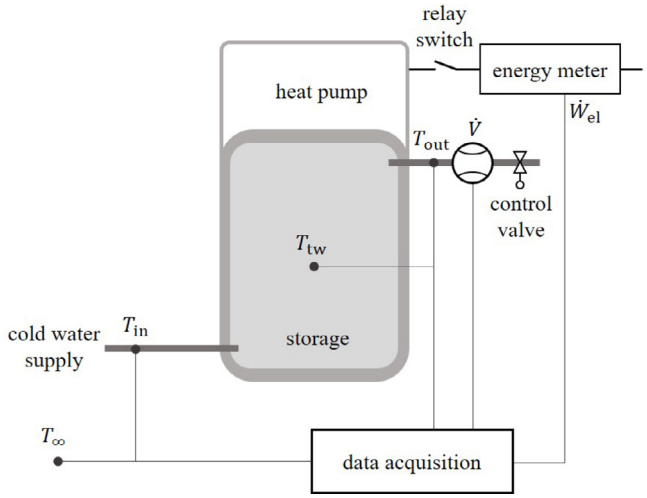

Fig. 1. Experimental setup including main components and sensor equipment.

based on the volume flow rate $\dot{V}$, the water inlet temperature T_{in}, and the water outlet temperature T_{out}, assuming a constant specific heat capacity of water $c_w = 4.180$ kJ/(kgK). The hot water demand profile is executed by a stepless-controllable 2-way motor valve (type Bürkert 3280 [30]). Data acquisition, demand control signal, and relays switch are carried out by the Gantner Instruments Q. station-XT [31]. Relay switching is necessary for transferring the optimal control signal u to the HP, by overruling the standard control setting.

3. Model predictive control approach

3.1. Thermal modelling and optimization problem

The MPC approach adapted from EHWHs [25] is presented in Fig. 2. It is based on a incentive driven linear optimization problem (LP) deduced by a single-node model of the HWHP's TES, considering temperature limits as linear constraints and assuming a predicted demand Q^*_{dem}. The model of the TES is based on an open system energy balance resulting in the following ordinary differential equation:

$$C\frac{d\bar{T}}{dt} = -\dot{Q}_{dem}(t) + COP \cdot \dot{W}_{el}(t) - \dot{Q}_{loss}(t), \tag{1}$$

where $COP \cdot \dot{W}_{el}$ represents the thermal heat input, $\dot{Q}_{loss}$ the losses to the environment, and $\dot{Q}_{dem}$ the DHW demand, defined as

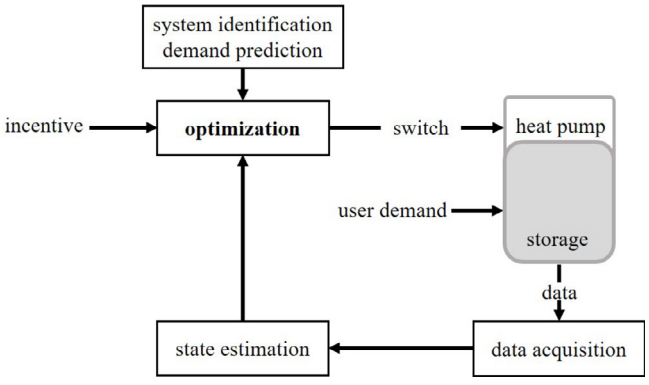

Fig. 2. Main processes and data streams of the MPC approach.

$$\dot{Q}_{dem}(t) = \dot{V}(t) \cdot \varrho \cdot c_w(T_{out} - T_{in}), \tag{2}$$

$$\dot{W}_{el}(t) = P_{el} \cdot u(t), \quad u(t) \in \{0, 1\}, \tag{3}$$

$$\dot{Q}_{loss}(t) = UA(\bar{T}(t) - T_\infty). \tag{4}$$

Here, $\dot{V}$ is the water volume flow, ϱ is the water density, c_w is the specific heat capacity of water, and UA is the overall heat transfer characteristics of the storage. Eq. (1) can be solved analytically by setting the initial condition $\bar{T}(t_0) = \bar{T}_0$, which leads to

$$\bar{T}(t) = \bar{T}_0 \cdot e^{\left(-\frac{UA}{C}(t-t_0)\right)} + \left(1 - e^{\left(-\frac{UA}{C}(t-t_0)\right)}\right)\left[\frac{COP \cdot \dot{W}_{el}}{UA} - \frac{\dot{Q}_{dem}}{UA} + T_\infty\right]. \tag{5}$$

Eq. (5) can be used to formulate the optimization problem by assuming piecewise constant values for $c(t), \dot{Q}_{dem}(t)$ and $\dot{W}_{el}(t)$ for a set of N time steps of a duration of Δt, i.e.,

$$\bar{T}(t_0 + i\Delta t) = \bar{T}(t_0) \cdot \lambda^i + \sum_{j=0}^{i-1}\left[(1-\lambda)\lambda^{i-j-1}\left(\frac{COP \cdot \dot{W}^{(j)}_{el}}{UA} - \frac{\dot{Q}^{(j)}_{dem}}{UA} + T_\infty\right)\right], \quad \lambda = e^{\left(-\frac{UA}{C}\Delta t\right)}. \tag{6}$$

Eq. (6) can be solved through an iterative process indicated by i and j for the defined set of N time steps.

Assuming a predicted demand Q^*_{dem}, the LP stated as cost minimization for DHW heating can be formulated as follows to find the optimal solution vector for switching the HP.

$$\begin{aligned} \left(u^{(1)}_{opt}, \cdots, u^{(N)}_{opt}\right) &= \min_{u^{(1)},\cdots,u^{(N)}} \sum_{i=0}^{N} c^{(i)} \cdot u^{(i)} \text{ s.t.} \\ T_{max} &\geqslant \bar{T}^{(j)} \forall j, \\ T_{min} &\leqslant \bar{T}^{(j)} \forall j : \dot{Q}^{(j)*}_{dem} > 0, \end{aligned} \tag{7}$$

where the storage temperature is kept below the set maximum temperature T_{max} and kept above the minimum temperature T_{min} during DHW draw-offs. Details of the LP formulation and the matrix notation can be found in Kepplinger et al. [25].

3.2. System identification and state estimation

According to Eq. (1), three system parameters are to be estimated: the total thermal capacitance C, the overall heat transfer characteristics UA, and the HP's coefficient of performance COP. The thermal capacitance is calculated from the known physical properties (water mass, temperature spread and specific heat capacity of water). The heat transfer characteristics and coefficient of performance are estimated using the prediction error method (PEM).

For identifying the system parameters UA and COP, the aim is to minimize the root mean squared error (RMSE) between approximated average storage temperature $\bar{T}$ and measured thermal well temperature T_{tw} for a given set of historical data at discrete points in time $t \in \mathcal{T}_{HC}$, as following:

$$\widetilde{UA}, \widetilde{COP} = \arg\min_{UA,COP} \sqrt{\frac{\sum_{t\in\mathcal{T}_{HC}} \left(\bar{T}(t) - T_{tw}(t)\right)^2}{|\mathcal{T}_{HC}|}}.$$

$\mathscr{T}_{\mathrm{HC}}$ specifies the set of points in time, where the measured thermal well temperature can be assumed to be a good estimate for the average storage temperature. Heating cycles (HC) are suitable time sets, since TES charging is considered as an aspect of de-stratification [26,32]. To assume an uniform temperature distribution in the TES, the thermal well temperature has to be close to the upper layer temperature. This is true, if the thermal well temperature exceeds the outlet temperature during the last draw event, representing the upper layer temperature.

To calculate the set $\mathscr{T}_{\mathrm{HC}}$ of points in time, which allow to assume a uniform temperature distribution, we follow the approach presented in [26]. The set is the join of the subsets of all heating cycles h,

$$\mathscr{T}_{\mathrm{HC}} = \bigcup_{h} [t_{\mathrm{on}}, t_{\mathrm{cool}}], \tag{9}$$

where the different points in time can be described as follows (cf. Fig. 3):

1. t_{on}: Start of heating cycle;
2. t_{uni}: Exceedance of thermal well temperature compared to the outlet temperature of the last prior demand marks point in time assuming nearly uniform temperature distribution;
3. t_{off}: End of heating cycle;
4. t_{cool}: End of cooling-off phase after the heating cycle and previous to the next DHW demand.

The PEM resulted in the parameters of $UA = 1.828$ W/K and $COP = 3.031$ with an $RMSE = 1.410$ K. The calculation of the thermal capacitance resulted in $C = 8.360 \cdot 10^5$ J/K.

During execution of the MPC, prior to each optimization, the average temperature of the TES has to be estimated (cf. Eq. (5)), which serves as initial condition of the model, cf. Eq. 7. Whenever a uniform temperature distribution according to the method described before can be assumed (cf. Eq. 9), the average temperature is assumed to be equal to the thermal well temperature. Otherwise, the model as described in Eq. 5 is used to calculate the average temperature forward in time considering the measured data (compressor power, temperatures of the surroundings, and hot water demand).

3.3. User scenarios

The DHW profiles by Ritchie et al. [24] are used to provide a base for comparison of HYS and MPC. Matching properties (household size, storage size and dimensions) of HWHPs and EHWHs enable the profile transfer to our work. An algorithm was developed to execute DHW profiles on the test rig. Hence, we have converted the profiles from the original quantity volume flow to energy, with a fixed draw-off temperature $T_{\mathrm{dem}} = 38$°C.

In the first scenario, we assume perfect foreknowledge of the DHW demand, referred to as perfect prediction (PP).

In a second scenario, we use the prediction according to the DDP method by Ritchie et al. [24].

By comparing both scenarios, we are able to evaluate how much of the perfect scenario's potential is achievable through a state-of-the art prediction method. Both profiles, the DDP and the actual user demand are compared cumulatively to show the prediction errors in Fig. 4.

3.4. Stock market price

As incentive function $c(t)$, the EXAA day-ahead stock market prices [33] of a typical winter week with 15-min resolution are used. The EXAA prices for the upcoming day are considered to be known at midnight.

3.5. Live routine

The whole framework including all algorithms is developed in *Python* language.

Sensor data is acquired at a resolution of 60 s and stored on the cloud-edge environment of Gantner Instruments [34]. The optimization routine works in a 15-min interval to find the best switching state by serving a prediction horizon up to 24 h dependent on the incentive available. Thereby, the average temperature as central element of decision making is repetitively calculated, using state estimation prior to the optimization. After optimization, the solution vector is executed to switch the HP unit accordingly.

The control framework given from the manufacturer poses two difficulties to overcome: a) delay until start of HP operation and b) operation in dead band.

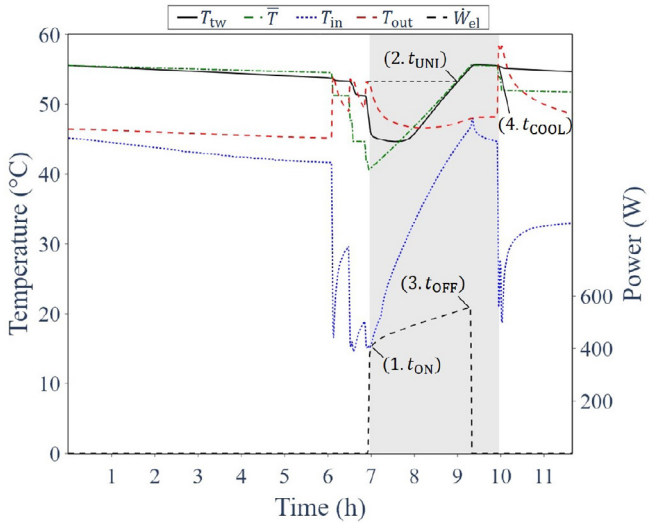

Fig. 3. System identification procedure according to Kepplinger [26].

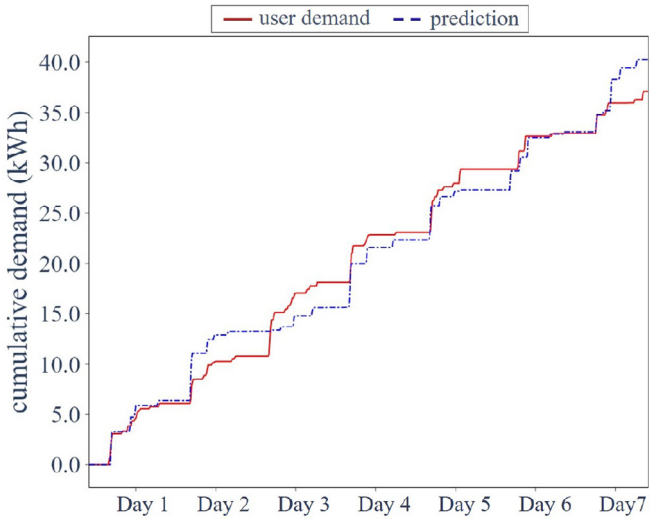

Fig. 4. Cumulative demand comparison of actual user demand and prediction.

1. To stabilize operation conditions, the manufacturer executes the fan operation before the actual compressor start. Hence, a pre-switching strategy is executed prior to the current optimization.
2. The hysteresis does not support the operation inside the temperature dead band until the lower threshold value is reached. To facilitate this unused potential, the control memory of the HP has to be reset by switching the HP off and on again.

4. Results and discussion

4.1. Analysis of MPC potential

To verify the MPC potential, experimental HWHP data of HYS and two MPC scenarios for a typical winter week are considered. The data are compared with respect to: 1) consumed electric energy, 2) total DHW demand, 3) coefficient of performance, 4) costs per unit electricity, 5) costs per unit heat, 6) total cost for electricity, 7) total operation time, and 8) HP start-ups, cf. Table 1.

In HYS mode the thermal well temperature $T_{tw,HYS}$ strives to the set temperature of $T_{max} = 55°C$ (cf. Fig. 6, subplot 3), whereas the average storage temperatures in both MPC modes are kept within the limits according to the optimization. In detail, this can be observed in Fig. 5, where the thermal well temperature $T_{tw,PP}$ matches closely the calculated average storage temperature $\overline{T}_{calc,PP}$. Hence, Fig. 6 (subplot 2) shows that in PP and DDP mode, the electrical power is predominantly consumed in local price minima, whereas in hysteresis mode it follows a clear demand dependent pattern. Consequently, compared to the hysteresis, the electrical input decreased by 19.50%, and 11.38% in PP and DDP mode, respectively. Additionally, the total operation time decreases by 32.78% (PP), and 22.01% (DDP), respectively, cf. Table 1. Thus, shorter operation times and less electricity consumption results in an efficiency increase of 24.07% (PP), and 12.70% (DDP), respectively. The costs per unit electricity decreased by 17.23% and 14.20%, the costs per unit heat by 33.29% and 23.86%, and the total cost for electricity by 33.37% and 23.96% for PP and DDP scenario, respectively, compared to the hysteresis.

Fig. 7 shows that especially in longer heating periods the execution of the given switching signal (blue) failed several times (red areas). The failure stems from the error in state estimation, as the energy input realized exceeds the one expected by the optimization.

While we achieve a reduction of electrical energy and cost in the realistic scenario by about 11.4%, and 24%, respectively, the reductions in literature range from 4 – 22% and from 7 – 34% [16,18,23]. For the COP, we achieve an increase of about 12.7%, literature reports values of 5 – 22% [16,18].

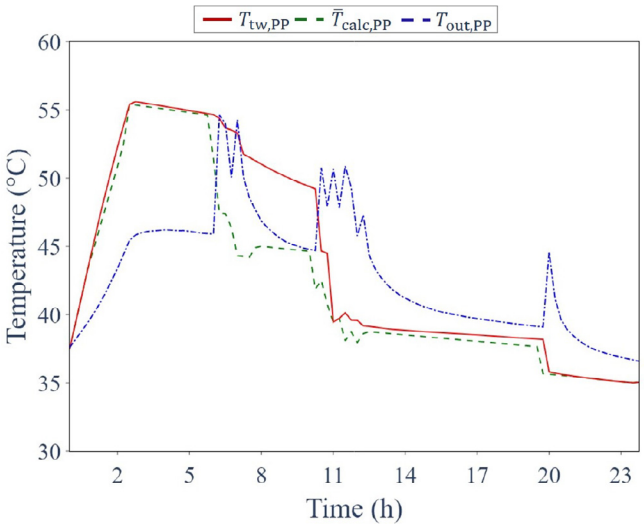

Fig. 5. Comparison of thermal well temperature and calculated average storage temperature for perfect prediction (PP).

4.2. Efficiency and comfort conditions

The COP increase of the MPC scenarios (cf. Table 1) can be analyzed by the following observations: Fig. 8 (left) shows the decline of the operation time per cycle, where the average operation time for the DDP and PP scenario decreases by about 40% compared to the hysteresis. In terms of power, the HP operates in a 3.4-times broader range and the lower quartile decreases down to about 280 W in the optimized cases, cf. Fig. 8 (right). Further observation in Fig. 9 (right) show the decline of the average thermal well temperature down to about 45°C and the increase of the interquartile range in the optimized cases. Hence, the comparison of the boxplots of Figs. 8 and 9 reveals how the decrease in operation time and power consumption results in lower thermal well temperatures.

The comparison of the interquartile range of both box plots, thermal well temperature and storage outlet temperature (cf. Fig. 9 (left and right)), shows that short heating cycles (cf. Fig. 8 (left)) can lead to stratification in the storage. Thus, by extension of the temperature band, thermal losses of the storage decrease compared to the higher temperature level in the hysteresis mode, and this inherently increases the efficiency of the storage [32].

However, through the extension of the temperature band, the lower quartile of the thermal well temperatures in the PP case (cf. Fig. 9 (right)) shows a violation of the minimum set-

Table 1
Aggregated experimental quantities for hysteresis (HYS) and MPC for the two scenarios: Perfect prediction (PP) and data-driven probabilistic prediction (DDP). For the DHW demand, a common week in winter is considered. Quantities from top to bottom: Consumed electric energy, total DHW demand, coefficient of performance, costs per unit electricity, costs per unit heat, total cost for electricity, total operation time and HP start-ups.

Parameter	HYS	PP	DDP	Rel. deviation (PP/DDP)
W_{el} (kWh)	19.32	15.55	17.13	−19.50%/ −11.38%
Q_{dem} (kWh)	37.15	37.10	37.10	−0.13%/ −0.13%
COP (−)	1.92	2.39	2.17	+24.07%/ +12.70%
C_{el} (€/MWh)	70.89	58.68	60.83	−17.23%/ −14.20%
C_{th} (€/MWh)	36.87	24.60	28.07	−33.29%/ −23.86%
$\sum C_{el}$ (€)	1.37	0.91	1.04	−33.37%/ −23.96%
Total operation time (h)	80.53	54.13	62.80	−32.78%/ −22.01%
HP start-ups (−)	15.00	30.00	29.00	+100.00%/ +93.34%

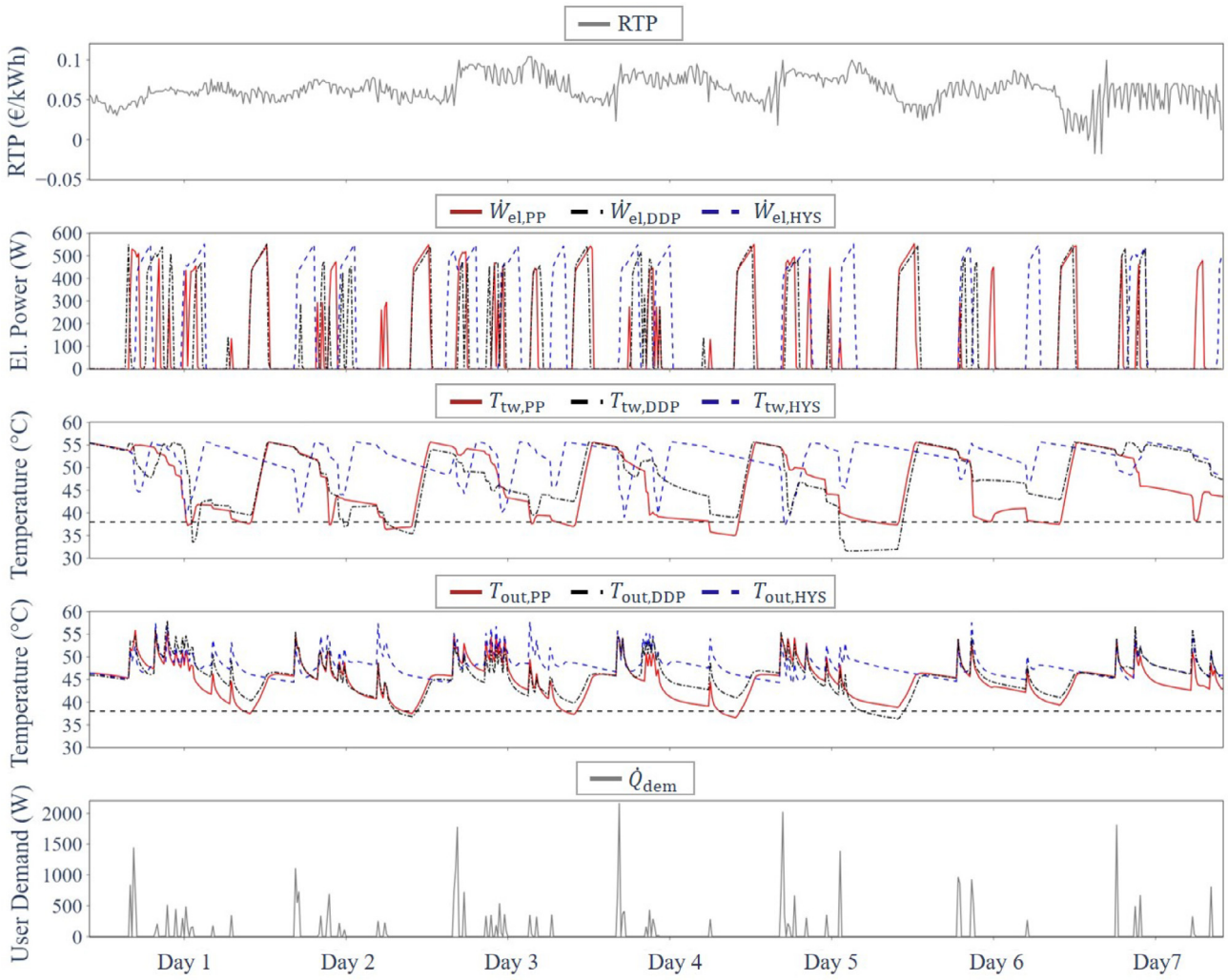

Fig. 6. Comparison of electrical power, thermal well and outlet temperatures for hysteresis (HYS), perfect prediction (PP) and data-driven probabilistic prediction (DDP).

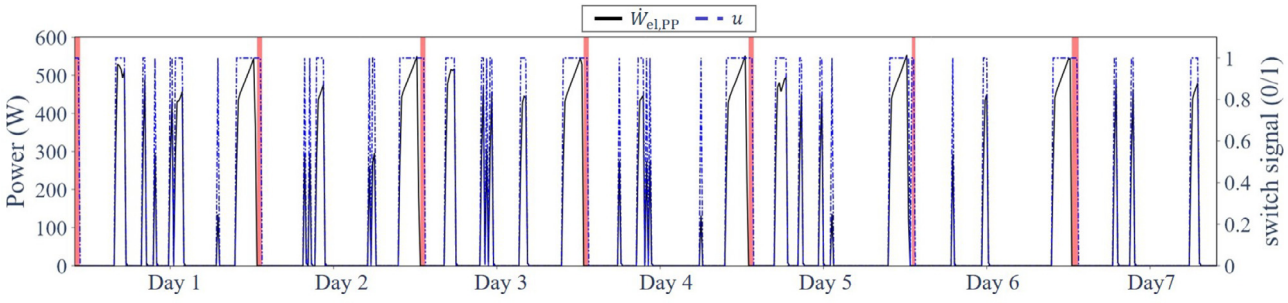

Fig. 7. Failed switching (red areas) compared to actual electrical power consumption (black) in the PP scenario.

temperature. As further noticed in Fig. 6 (subplot 3), the thermal well temperatures drop below the minimum set-temperature in both MPC modes. While the thermal well temperature gives a first insight of the temperature in the storage, the storage outlet temperature is the important quantity to assess the user's comfort. The storage outlet temperature represents the draw-off temperature experienced by the user. Fig. 6 (subplot 4) and Fig. 9 (left) show that user's comfort is maintained at all times as the outlet temperatures stay above the set-temperature limit of $T_{min} = 38°C$. The results proof the capability of the MPC strategy to shift loads and save costs, while maintaining user comfort.

5. Conclusions

Heat pumps with thermal energy storages can provide additional flexibility for renewable energy integration through their ability to shift loads. In multi-family residential complexes, where the rules regarding *Legionella* are strict, decentralized heat pump

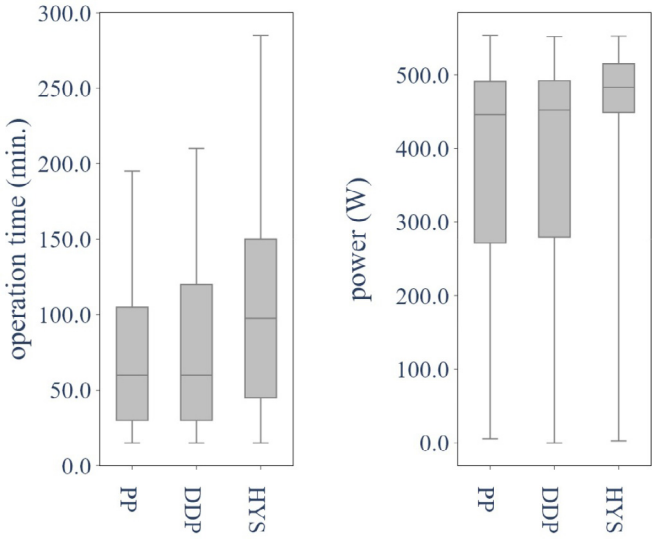

Fig. 8. Comparison of hysteresis (HYS), perfect prediction (PP) and DDP prediction (DDP) scenario for: Operation time (left) and power consumption (right).

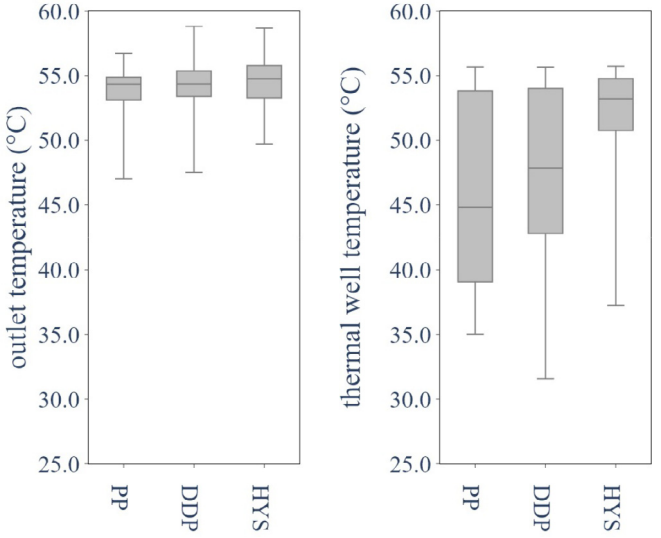

Fig. 9. Comparison of hysteresis (HYS), perfect prediction (PP) and DDP prediction (DDP) scenario for: outlet temperature (left) and thermal well temperature (right).

systems for DHW supply can provide a viable solution. However, to this day, experimental studies with model predictive control approaches considering solely domestic hot water use have not been available.

Therefore, we showed for the first time, how state-of-the-art approaches (MPC, system identification, live state estimation, and demand prediction) can be transferred from electric hot water heaters (EHWH) to hot water heat pumps (HWHP), combined, and deployed in a real-world HWHP setup. We applied the system identification method, to be able to determine the best parameter set of the model. The automated state estimation method stabilized the routine by reducing modelling errors during live operation. As the demand and it's prediction are crucial for thermal energy storage management, where the utilisation of the flexibility lays within, our realistic demand prediction method was key to enable realistic achievable scenarios.

We also provide results for the significant MPC potential of DHW use with HPs compared to the standard hysteresis control.

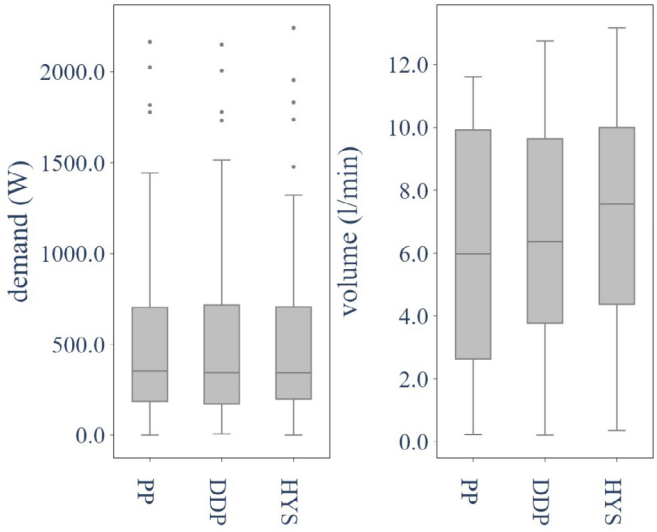

Fig. A.10. Comparison of hysteresis (HYS), perfect prediction (PP) and DDP prediction (DDP) scenario for: DHW demand (left) and draw-off volume (right).

Decreased electric energy demand, electricity cost, and increased energy efficiency, have been achieved in a realistic experimental setting, while maintaining the user's comfort at all times. The experimental results quantify and validate the savings, as well as the DSM potential, achievable by a state-of-the-art prediction method in two prediction scenarios. In the perfect scenario, a decrease in costs per unit electricity and electric energy of 17.2% and 19.5%, respectively, as well as an increase of the COP of 24.1% was achieved. For the realistic scenario the costs per unit electricity and electric energy decreased by 14.2% and 11.4%, respectively, while the COP increased by 12.7%. By accounting for higher stratification in the TES, cost and energy savings could be attainable by adaption to a multi-node model as suggested in [26].

Further, the experimental implementation revealed challenges of the interaction with the HP's local controller and the fixed manufacturer settings. For further work with similar experimental setups, scientists might face the same problems and should pay attention to these.

CRediT authorship contribution statement

Christian Baumann: Conceptualization, Methodology, Software, Validation, Formal analysis, Investigation, Data curation, Writing - original draft, Visualization. **Gerhard Huber:** Conceptualization, Methodology, Writing - review & editing. **Jovan Alavanja:** Software. **Markus Preißinger:** Writing - review & editing, Funding acquisition. **Peter Kepplinger:** Conceptualization, Methodology, Resources, Writing - review & editing, Supervision, Project administration.

Data availability

Data will be made available on request.

Declaration of Competing Interest

The authors declare that they have no known competing financial interests or personal relationships that could have appeared to influence the work reported in this paper.

Acknowledgements

The financial support by the Austrian Federal Ministry for Digital and Economic Affairs and the National Foundation for Research, Technology and Development and the Christian Doppler Research Association is gratefully acknowledged. We thank Gantner Instruments for providing the hardware, as well as the help on interfacing with it. We thank Dr. Michael Ritchie of the University of Stellebosch for the feedback and discussions on his prediction method and the profile generator.

Appendix A. .

Fig. A.10

References

[1] European Heat Pump Association, Market Report 2021 – EHPA. URL:https://www.ehpa.org/market-data/market-report-2021/, accessed 2022-09-01.
[2] D. Fischer, H. Madani, On heat pumps in smart grids: A review, Renewable and Sustainable Energy Reviews 70 (2017) 342–357, 00005. doi:10.1016/j.rser.2016.11.182.
[3] Bundesverband Wärmepumpe e.V., Starkes Wachstum im Wärmepumpenmarkt. URL:https://www.waermepumpe.de/presse/pressemitteilungen/details/starkes-wachstum-im-waermepumpenmarkt/, accessed 2022-09-01
[4] A. Arteconi, N. Hewitt, F. Polonara, State of the art of thermal storage for demand-side management, Appl. Energy 93 (2012) 371–389, https://doi.org/10.1016/j.apenergy.2011.12.045.
[5] M. Killian, M. Kozek, Ten questions concerning model predictive control for energy efficient buildings, Build. Environ. 105 (2016) 403–412, https://doi.org/10.1016/j.buildenv.2016.05.034.
[6] J. Clauß, C. Finck, P. Vogler-Finck, P. Beagon, Control strategies for building energy systems to unlock demand side flexibility – A review, in: IBPSA Building Simulation, San Francisco, 2017, pp. 1–10, URL:http://hdl.handle.net/10197/9016.
[7] T.Q. Péan, J. Salom, R. Costa-Castelló, Review of control strategies for improving the energy flexibility provided by heat pump systems in buildings, J. Process Control 74 (2019) 35–49, https://doi.org/10.1016/j.jprocont.2018.03.006.
[8] D. Fischer, J. Bernhardt, H. Madani, C. Wittwer, Comparison of control approaches for variable speed air source heat pumps considering time variable electricity prices and PV, Appl. Energy 204 (2017) 93–105, https://doi.org/10.1016/j.apenergy.2017.06.110.
[9] S. Bechtel, S. Rafii-Tabrizi, F. Scholzen, J.-R. Hadji-Minaglou, S. Maas, Influence of thermal energy storage and heat pump parametrization for demand-side-management in a nearly-zero-energy-building using model predictive control, Energy Build. 226 (2020), https://doi.org/10.1016/j.enbuild.2020.110364.
[10] C. Verhelst, F. Logist, J. Van Impe, L. Helsen, Study of the optimal control problem formulation for modulating air-to-water heat pumps connected to a residential floor heating system, Energy Build. 45 (2012) 43–53, https://doi.org/10.1016/j.enbuild.2011.10.015.
[11] M.U. Kajgaard, J. Mogensen, A. Wittendorff, A.T. Veress, B. Biegel, Model predictive control of domestic heat pump, in, American Control Conference, IEEE, Washington, DC 2013 (2013) 2013–2018, https://doi.org/10.1109/ACC.2013.6580131.
[12] F. D'Ettorre, M. De Rosa, P. Conti, D. Testi, D. Finn, Mapping the energy flexibility potential of single buildings equipped with optimally-controlled heat pump, gas boilers and thermal storage, Sustain. Cities Soc. 50 (2019), https://doi.org/10.1016/j.scs.2019.101689.
[13] J. Joe, P. Karava, A model predictive control strategy to optimize the performance of radiant floor heating and cooling systems in office buildings, Appl. Energy 245 (2019) 65–77, https://doi.org/10.1016/j.apenergy.2019.03.209.
[14] X. Jin, J. Maguire, D. Christensen, Model predictive control of heat pump water heaters for energy efficiency, in: Proceedings of the 18th ACEEE Summer Study on Energy Efficiency in Buildings, Pacific Grove, CA, USA, 2014, pp. 21–26.
[15] E.M. Wanjiru, S.M. Sichilalu, X. Xia, Model predictive control of heat pump water heater-instantaneous shower powered with integrated renewable-grid energy systems, Appl. Energy 204 (2017) 1333–1346, https://doi.org/10.1016/j.apenergy.2017.05.033.
[16] S. Kuboth, F. Heberle, T. Weith, M. Welzl, A. König-Haagen, D. Brüggemann, Experimental short-term investigation of model predictive heat pump control in residential buildings, Energy Build. 204 (2019), https://doi.org/10.1016/j.enbuild.2019.109444.
[17] S. Kuboth, T. Weith, F. Heberle, M. Welzl, D. Brüggemann, Experimental Long-Term Investigation of Model Predictive Heat Pump Control in Residential Buildings with Photovoltaic Power Generation, Energies 13 (22) (2020) 6016, https://doi.org/10.3390/en13226016.
[18] T. Pean, R. Costa-Castello, E. Fuentes, J. Salom, Experimental Testing of Variable Speed Heat Pump Control Strategies for Enhancing Energy Flexibility in Buildings, IEEE Access 7 (2019) 37071–37087, https://doi.org/10.1109/ACCESS.2019.2903084.
[19] H. Willem, Y. Lin, A. Lekov, Review of energy efficiency and system performance of residential heat pump water heaters, Energy Build. 143 (2017) 191–201, https://doi.org/10.1016/j.enbuild.2017.02.023.
[20] M. Obi, C. Metzger, E. Mayhorn, T. Ashley, W. Hunt, Nontargeted vs. Targeted vs. Smart Load Shifting Using Heat Pump Water Heaters, Energies 14 (22) (2021) 7574, https://doi.org/10.3390/en14227574.
[21] P. Kepplinger, Autonomous Demand Side Management of Domestic Hot Water Heaters, Dissertation, University of Innsbruck, Innsbruck, Austria, 2019.
[22] M.J. Ritchie, Usage-Based Optimal Energy Control of Residential Water Heaters, Dissertation, Stellenbosch University (2021), https://doi.org/10.13140/RG.2.2.12747.31524.
[23] P. Kepplinger, G. Huber, J. Petrasch, Field testing of demand side management via autonomous optimal control of a domestic hot water heater, Energy Build. 127 (2016) 730–735, https://doi.org/10.1016/j.enbuild.2016.06.021.
[24] M. Ritchie, J. Engelbrecht, M. Booysen, A probabilistic hot water usage model and simulator for use in residential energy management, Energy Build. 235 (2021), https://doi.org/10.1016/j.enbuild.2021.110727.
[25] P. Kepplinger, G. Huber, J. Petrasch, Autonomous optimal control for demand side management with resistive domestic hot water heaters using linear optimization, Energy Build. 100 (2015) 50–55, https://doi.org/10.1016/j.enbuild.2014.12.016.
[26] P. Kepplinger, G. Huber, M. Preißinger, J. Petrasch, State estimation of resistive domestic hot water heaters in arbitrary operation modes for demand side management, Therm. Sci. Eng. Progr. 9 (2019) 94–109, https://doi.org/10.1016/j.tsep.2018.11.003.
[27] Austria Email GmbH, Produktinformationen Trinkwasserwärmepumpe EXPLORER EVO 2 – Austria Email GmbH. URL:https://www.austria-email.de/produkte/waermepumpensysteme/waermepumpen-trinkwasser/explorer-evo-2/, accessed 2022-09-01.
[28] Lumel, Produktinformationen Messgerät Lumel N27P. URL:https://www.lumel.de, accessed 2022-09-01.
[29] ifm electronic, Produktinformationen Magnetisch-induktiver Durchflusssensor SM6000 – ifm. URL:https://www.ifm.com/at/de/product/SM6000, accessed 2022-09-01.
[30] Bürkert, Produktinformationen 2-Wege-Motorventil Typ 3280 - Bürkert. URL: https://www.buerkert.at/de/type/3280, accessed 2022-09-01.
[31] Gantner Instruments, Produktinformationen Q.station XT - Gantner Instruments. URL:https://www.gantner-instruments.com/de/products/controller/q-station-x/, accessed 2022-09-01.
[32] J. Fernández-Seara, F.J. Uhía, J. Sieres, Experimental analysis of a domestic electric hot water storage tank. Part II: dynamic mode of operation, Appl. Therm. Eng. 27 (1) (2007) 137–144, 00038. doi:10.1016/j.applthermaleng.2006.05.004.
[33] Energy Exchange Austria, Day-Ahead Preisdaten – Historische Marktdaten Energy Exchange Austria. URL:https://www.exaa.at/marktdaten/historische-marktdaten/, accessed 2022-09-01.
[34] Gantner Instruments, Produktinformationen GI.cloud – Dezentrale Streaming-Plattform von Gantner Instruments. URL:https://www.gantner-instruments.com/products/data-acquisition-software/gi-cloud/, accessed 2022-09-01.